Journal of Natural Gas Science and Engineering 100 (2022) 104471

Contents lists available at ScienceDirect

Journal of Natural Gas Science and Engineering

journal homepage: www.elsevier.com/locate/jngse

Characterization of the mud displacement in an enlarged wellbore: An integrated rock-fluid model

Yuxing Wu [a,*], Saeed Salehi [a], Mahmoud Khalifeh [b]

[a] Mewbourne School of Petroleum and Geological Engineering, University of Oklahoma, USA
[b] Department of Energy and Petroleum Eng., Faculty of Science and Technology, University of Stavanger, Norway

ARTICLE INFO

Keywords:
Mud displacement
Enlarged wellbore
Washout
Mud contamination
Geopolymer

ABSTRACT

Cement-mud displacement plays a crucial role in the sealability of cement sheaths. Irregular geometric features of a wellbore due to washout can have a negative impact on mud and cement mobilization. An unstable interface between two fluids always leads to mud channeling, interfluid mixing, and cement contamination, degrading the cement quality. Many factors, such as mechanical and rheological properties of fluids, annulus geometry, flow pattern, and flow rate, significantly influence the displacement efficiency. This study investigates the characterization of the mud displacement in an irregular horizontal well using a 3D computational fluid dynamics (CFD) model. Mud is displaced in an enlarged wellbore by geopolymer and neat class G cement. The wellbore geometry is developed based on the caliper log data from an unconventional shale well in the Tuscaloosa Marine Shale (TMS) lithology. The effects of pump rate, density difference, and mud contamination are evaluated by numerical simulations. The results present those residual muds mainly exist in the upper annulus of the enlarged section. Geopolymer has a better sealing performance and can resist more water-based mud (WBM) contaminations than neat class G cement. The scenario with a low mud-cement density difference and high cement injection rate results in a high cement volume fraction, mitigating the gas migration.

1. Introduction

Cement sheath is an impermeable material acting as an important barrier to prevent unintended fluid/gas communications in the wellbores. An excellent cement system is expected to provide casing supports, producing zone isolations and leakage preventions. Poor quality of cement can lead to well integrity issues and negative impacts on environments and human safety, such as casing damage, blowout, groundwater contaminations, and greenhouse gas leakage. The process of mud displacement plays a significant role in the quality of hardened cement (Enayatpour and van Oort, 2017; Foroushan et al., 2020). After setting a casing into an openhole, the cement slurry is pumped to a target depth to displace original drilling fluids (mud) in the annulus. Through the hydration mechanism, the cement is transformed from slurry to solid, developing a hardened cement. Previous studies have presented that proper density, rheology, and operational strategy designs are beneficial to improve the mechanical and bonding strength of cement.

During the drilling process, a proper density design of the drilling mud establishes a stable borehole by counterbalancing formation pressure (i.e., avoiding formation fluids influx, like blowout) and preventing the uncased openhole collapse. However, satisfaction with the drilling requirements does not mean that the mud is beneficial to the cementing. Bu et al. (2016) investigated the mud removal in high deviated wells using numerical simulations. The cement slurry directly removed drilling fluid in the eccentric and inclined wells. Cement systems with different density ratios were applied in the model. The cement slurry density was variable, while the other fluid properties remained constant. The interface was assumed steady, and no mixing and diffusion were considered at the mud-cement interface. For the eccentric wells with an inclination angle of 75°, if the density difference was low (i.e., 0–0.4 g/cm^3 in the study), a higher eccentricity resulted in an inefficient displacement. When the density difference was high, no correlation was presented. The level of casing eccentricity highly determined the optimal density difference. The study of the effect of inclination angle showed no significant influence if the system had lower density difference, while as the density difference increased, lower inclination angles would have a better performance. In general, the density difference of the displacing and displaced fluids affects the cement distribution at the mud-cement interface due to gravity effects (Savery et al., 2007; Dutra et al., 2004).

* Corresponding author.
E-mail address: yuxingwu@ou.edu (Y. Wu).

https://doi.org/10.1016/j.jngse.2022.104471
Received 16 August 2021; Received in revised form 5 February 2022; Accepted 9 February 2022
Available online 11 February 2022

Rheological properties such as apparent viscosity, yield point, and gel strength are another nature to ensure a successful well construction. A proper design should provide enough energy to transfer the rock fragments to the surface and inhibit filter cake development (Lavrov and Torsaeter, 2016). Many factors have been proved to influence the rheological properties, such as temperature, the types of mud and cement, petroleum fluids additives, and contaminations during the mud displacement. Eid et al. (2021) tested the rheological properties of rock-based geopolymer and neat class G cement with different amounts of water- (WBM) and oil-based muds (OBM). All cement slurries were followed the Herschel-Bulkley non-Newtonian rheological model as their viscosity decreased with an escalation in shear rate. For the geopolymers, more WBM and OBM contaminations resulted in low shear stress, especially at a high shear rate due to the electrokinetic potential of the geopolymeric slurry (Liu et al., 2019). The influence of WBM was more sensitive than OBM. Both WBM and OBM reduced the viscosity profile of geopolymers. For the class G cement, the shear stress was reduced by WBM contamination, while OBM could cause the increase of the shear stress. In general, mud contaminations reduce the strength of the cement after hardening (Li et al., 2016).

Operational factors are also recognized as a major consideration in cementing job design. Early research highlighted that displacing rate could affect the displacement process seriously. Richard and Crook (1979) compared cement displacing mud with different flow rates in a vertical wellbore. The flow rate from high to low separated the fluid flow into three regimes – turbulent, laminar, and plug regimes. High flow rates in turbulent and laminar regimes provided a better displacement than plug flow rates. Martin and Latil (1978) conducted further research and observed that a high flow rate in a turbulent regime was beneficial to the displacement and mitigated the hole cleaning issues (Moroni et al., 2009; Pang et al., 2018, 2019). However, achieving a turbulent flow regime during cement with cement slurry may not be doable. The high flow rate may be incompatible with the limitation that exceeds the admissible annular pressure, exceeding the equivalent circulating density (ECD). The determination of the optimum pumping rate should also consider annulus geometry, pipe eccentricity, drilling fluid and cement slurry types, and pipe movement. For the eccentric pipe, cement slurry tended to flow through the wide-side annulus with a high flow rate to

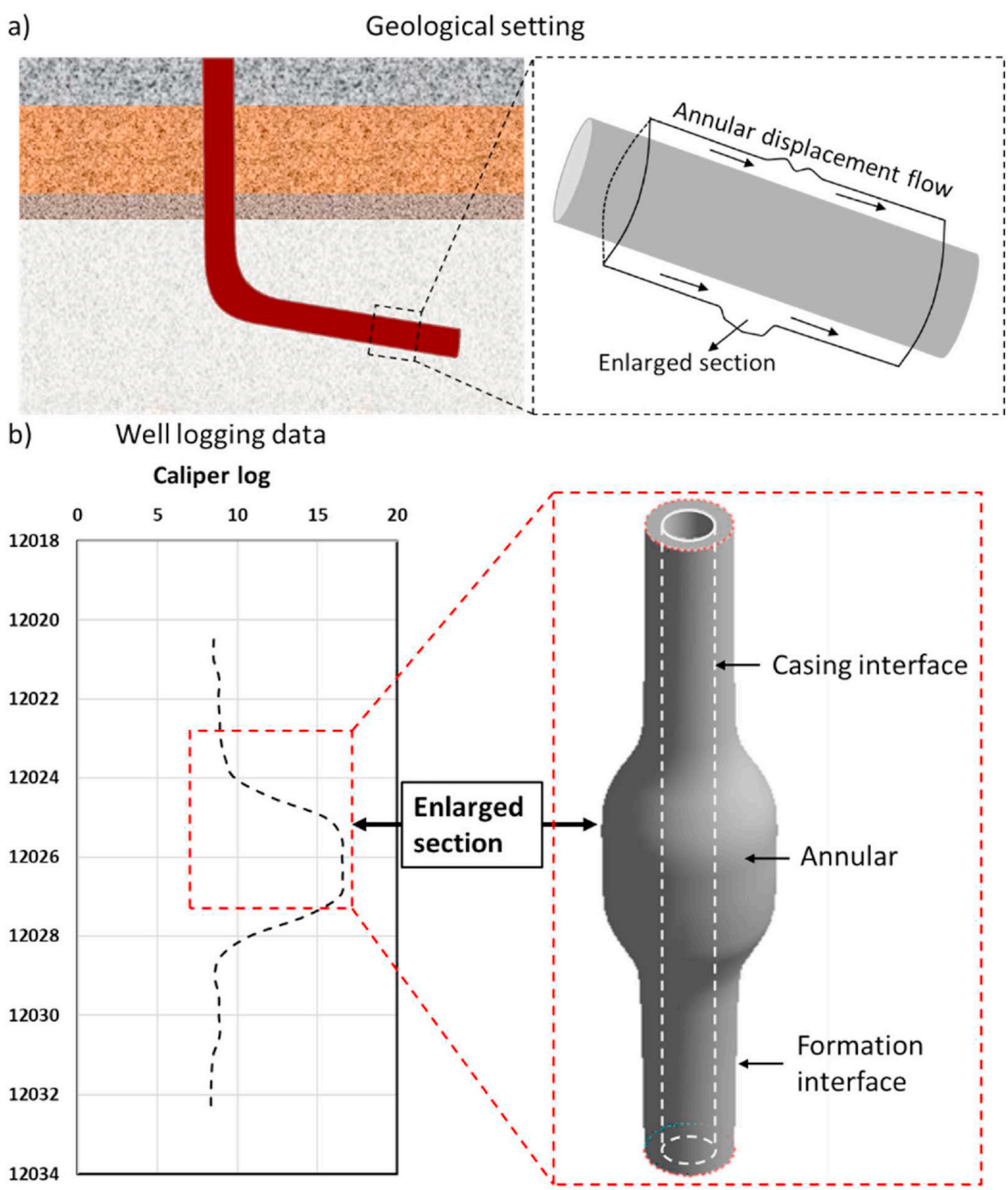

Fig. 1. a) Washout (enlarged) section of an annulus; b) Caliper log of TMS from 12020.5 ft to 12032.5 ft.

provide a better displacement behavior, while for the narrow-side, the resistance of fluid flow was high and the slurry was through the annulus with a low rate to decrease the displacement efficiency or bypassed the annulus (Xie et al., 2015; Xu et al., 2020). Pipe rotation is applied as a remedial operation to mitigate the negative impacts of non-ideal conditions, such as casing eccentricity, improper mud, and cement properties. The rotation enhances mud displacement by the improvement of hole cleaning (Bittleston and Hassenger, 1992; Ozbayoglu et al., 2008; Yeu et al., 2019) and increases the pumpability of cement slurry, especially in the narrow-side annulus of the eccentricity (Moroni et al., 2009; Enayatpour and van Oort, 2017; Guzman et al., 2018). However, the pipe rotation method is not always feasible due to high frictions in deviated wells and long lateral length (Livescu and Craig, 2017; Turner et al., 2019).

Besides operational factors, drilling fluid, and cement slurry types, the wellbore geometry is a primary factor influencing mud removal. Ideally, the borehole size should be the same as the size of the drilling bit. However, due to breakout, washout, and erosion, the wellbore is usually enlarged (Fig. 1). The enlarged wellbore has a negative impact on hole cleaning due to the reduction of mud flow rate (Kiran et al., 2019). A WBM displaced by neat class G experiment presented that in horizontal wells, the lowest quality cement segments were at the top of the enlarged annulus. Savery et al. (2007) developed a 3D mud displacement model to simulate the displacement near the reducing-size annulus due to the casing coupling protrusion. High fluid velocity was at the narrow segment of the annulus resulting in a better displacement efficiency. Renteria et al. (2019) investigated the impacts of irregular wellbore shape on the mud removal of the high deviated wells. In the horizontal section, the cement slurry tended to flow at the bottom because of the density difference, while casing eccentricity led to the cement displacing more mud in the wide side of the annulus than in the thin side. In the inclination sections, residual muds were left in the washout section during the displacement of high yield stress muds.

In this study, the performance of drilling fluid displaced by cement slurry is simulated using a 3D numerical model via a computational fluid dynamics (CFD) approach. The model is developed based on the real caliper log from a wellbore in the TMS, a weak shale resulting in an enlarged wellbore geometry by washout. The objective of the paper is to i) investigate the mud displacement performance in an enlarged wellbore based on the caliper log, ii) study the influence of mud-cement density difference, injection rate, and WBM contamination, and iii) compare the performance of geopolymer and neat class G.

2. Methodology

A 3D CFD model is developed to simulate the mud displacement performance in an irregular annular based on a real caliper log using commercial software, ANSYS FLUENT 2019 R2. Mass, momentum, laminar, and energy conservations of the system have been considered. The performance of neat class G cement and rock-based geopolymer are compared for investigating the displacement performance in an enlarged annulus between casing and formation. The geometry of the annulus is depicted based on the well logging data from the TMS. Since the allowable ECD is low due to the weakness of the formation, the mud is assumed to be injected in the laminar flow regime with low flow rates. Effects of density ratio, cement injection rate, and WBM contamination are also evaluated for finding the influenced parameter. Following assumptions are applied during the simulation:

- Drilling fluids are directly displaced by cement slurries. No spacer or other fluids are considered.
- Cement slurries with uniform velocity are injected into the inlet as a displacing fluid.
- The displacement process is steady. The circumferential velocity is not considered.
- Behaviors of drilling fluids and cement slurries follow the Herschel-Bulkley rheological theory.
- According to the calculated Reynolds number, all fluids follow the laminar mode (see the next section)
- Effects of the chemical interactions between drilling fluids and cement slurries are not considered. The quality of the cementing job depends on the cement volume fraction.
- The material properties used in this model are assumed constant if the change is not mentioned.

2.1. Governing equations

In this study, the fluid flow regime within the pipe is based on Reynolds number. When the number is less than 2300, the flow is referred to as a laminar flow. Between 2300 and 4000 is identified as a transient flow, and higher than 4000 is turbulent flow. Reynolds number is calculated by **Equation (1)**. Cement slurries are identified as displacing fluid. As the low injection rate applied in this study, all the fluids follow the laminar flow theory.

$$R_e = \frac{\rho v (D_1 - D_2)}{\mu} \tag{1}$$

where Re is Reynolds number. ρ, v, μ are density, velocity, and dynamic viscosity of the fluid. (D_1-D_2) is the size of the annulus.

According to Liao et al. (2003) and Bu et al. (2016), the shear stress of cement slurries and drilling fluids can be expressed as **Equation (2)** and **3.**

$$\tau_c = \left(\frac{\partial p}{\partial z} + \rho_c g cos\theta\right) y \tag{2}$$

$$\tau_m = \left(\frac{\partial p}{\partial z} + \rho_m g cos\theta\right) y + (\rho_c - \rho_m) g a cos\theta \tag{3}$$

where τ_c and τ_m are the shear stress of cement slurry and drilling fluid. ρ_c and ρ_m indicate the density of cement slurry and drilling fluid. $\frac{\partial p}{\partial z}$ represents friction pressure gradient between fluid and annulus surface. a is the distance between the slurry-mud interface to Z-axis. y refers to y-axis. θ is the inclination angle. For horizontal wells, θ equals to 90°.

The Herschel-Bulkley theory is used to control the rheological characterizations of cement slurries (**Equation (4)**) and drilling fluids (**Equation (5)**).

$$\begin{cases} \tau_c = \tau_{oc} \ (\tau_c \le \tau_{oc}) \\ \tau_c = \tau_{oc} + K_c \left(\left|\frac{dV_C}{dy}\right|\right)^{n_c} \ (\tau_c > \tau_{oc}) \end{cases} \tag{4}$$

$$\begin{cases} \tau_m = \tau_{om} \ (\tau_m \le \tau_{om}) \\ \tau_m = \tau_{om} + K_m \left(\left|\frac{dV_m}{dy}\right|\right)^{n_m} \ (\tau_m > \tau_{om}) \end{cases} \tag{5}$$

where τ_{oc} and τ_{om} are yield stresses of cement slurry and drilling fluids, respectively. K_c and K_m refer to consistency coefficient of cement and drilling fluids. $\frac{dV_c}{dy}$ and $\frac{dV_m}{dy}$ are velocity of slurries and muds at different location along the y-direction. n_c and n_m represent liquidity index, and V_c and V_m indicate axial velocity of cement and mud.

Then, Equations 4 and 5 equal to Equations 6 and 7:

$$\tau_{oc} + K_c\left(-\frac{dV_c}{dy}\right)^{n_c} = \left(\frac{\partial p}{\partial z} + \rho_c g cos\theta\right)y, 0 \le y < a \tag{6}$$

$$\tau_{om} + K_m\left(-\frac{dV_m}{dy}\right)^{n_m} = \left(\frac{\partial p}{\partial z} + \rho_m g cos\theta\right)y + (\rho_c - \rho_m) g a cos\theta, \quad a \le y < \frac{h}{2} \tag{7}$$

$$\text{At} \quad V_c|_{y=a} = V_m|_{y=a}, \quad V_m|_{y=\frac{h}{2}} = 0 \tag{8}$$

where h is the size of annulus, and $\frac{h}{2}$ is the middle of annulus.

Thus, the axial velocity of drilling fluid and cement slurry can be described as Equations 9 and 10.

$$V_c = \frac{n_c}{A(n_c+1)}\left[\left(Aa - \frac{\tau_{oc}}{K_c}\right)^{\frac{n_c+1}{n_c}} - \left(Ay - \frac{\tau_{oc}}{K_c}\right)^{\frac{n_c+1}{n_c}}\right] + \frac{n_m}{B(n_m+1)}\left\{\left[\frac{Bh}{2} + C\right]^{\frac{n_m+1}{n_m}} - [Ba + C]^{\frac{n_m+1}{n_m}}\right\} \tag{9}$$

$$V_c = \frac{n_m}{B(n_m+1)}\left\{\left[\frac{Bh}{2} + C\right]^{\frac{n_m+1}{n_m}} - [By + C]^{\frac{n_m+1}{n_m}}\right\} \tag{10}$$

where

$$\begin{cases} A = \dfrac{1}{K_c}\left(\dfrac{\partial p}{\partial z} + \rho_c g cos\theta\right) \\ B = \dfrac{1}{K_m}\left(\dfrac{\partial p}{\partial z} + \rho_m g cos\theta\right) \\ C = \dfrac{g a cos\theta}{K_m(\rho_c - \rho_m)} - \dfrac{\tau_{om}}{K_m} \end{cases} \tag{11}$$

2.2. Model Configurations

In this paper, a 3D numerical model is developed to estimate the cement quality of an irregular annulus. By applying pressure implicit method with splitting of operators (PISO) algorithm, pressure-velocity coupling in the flow region is acquired. The second-order upwind differencing scheme using multi-dimensional linear reconstruction is adopted to solve Navier-Stokes equations for describing the motion of viscous fluid substances. The convergence is deemed to be reached when the scaled residuals are less than 10^{-5} for energy, velocity, and continuity.

Based on the laminar flow theory, cement slurries remove drilling fluids in a horizontal casing-formation annulus. The inner diameter is 10 inches (254 mm). Although casing eccentricity would have a remarkable influence on the displacement, the aim of this investigation is the exploration of the optimized fluid selection and operational factor. The casing is assumed concentric. The outer diameter is generated based on a well in the TMS. According to the caliper log, the well depth from 12020.5 ft (3663.85 m) to 12032.5 ft (3667.51 m) is simulated due to the existence of an enlarged zone (Fig. 2). A mesh size of 5 mm is applied to provide enough accuracy of the results.

2.3. Material properties and boundary conditions

Fig. 3 illustrates the relationship between shear stress and shear strain for geopolymer and neat class G cement, measured using laboratory rheology tests. The property can be expressed using the Herschel-

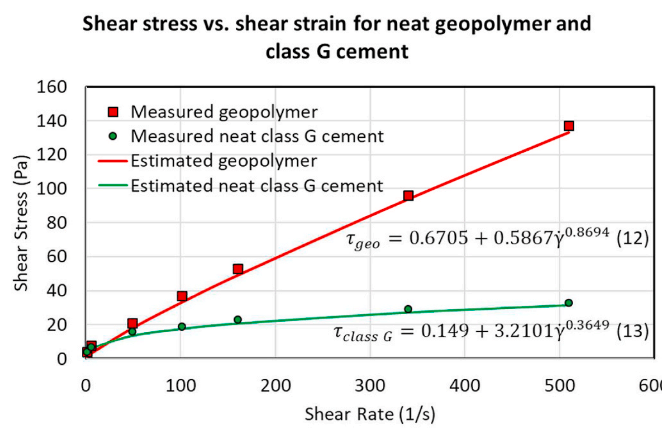

Fig. 3. Relationship between shear stress and shear rate of geopolymer and neat class G cement from laboratory measurements and Herschel-Bulkley estimations.

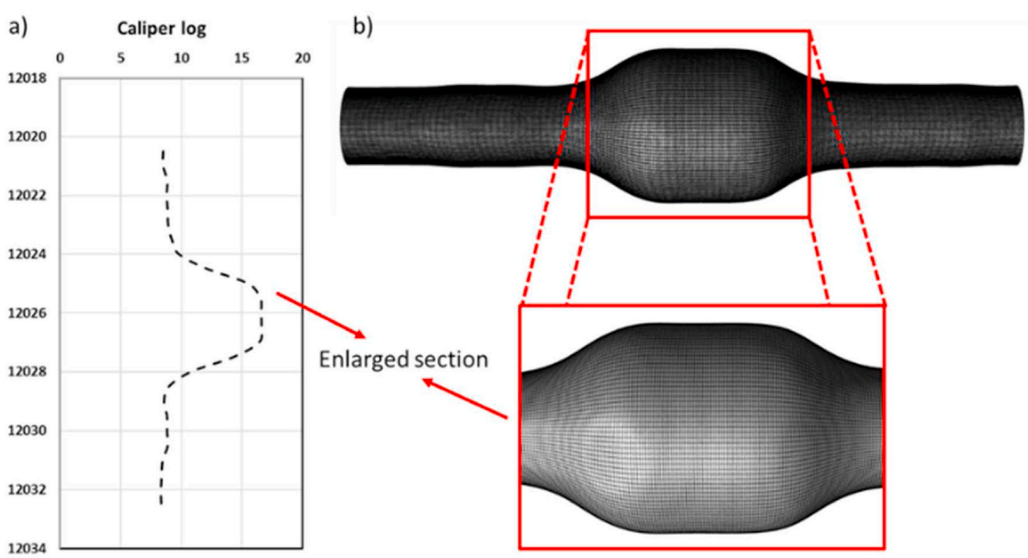

Fig. 2. a) Caliper log of one well in TMS from 12020.5 ft to 12032.5 ft; b) Model geometry with mesh.

Table 1
The properties of cement slurries and drilling muds.

Properties	Water based mud	Neat class G cement	Neat Geopolymer
Density (kg/m^3)	1234.25	2160.00	1970.00
Yield shear stress (Pa)	0.85	0.149	0.6705
Consistency coefficient ($Pa\bullet s^n$)	1.5	3.2101	0.5867
Liquidity index	7.5	0.3649	0.8694

Bulkley model, $\tau = T_0 + k\dot{r}^n$, where τ is shear stress, T_0 is yield stress, k is consistency coefficient, $\dot{r}$ is shear rate, and n is liquidity index (Fig. 3: **Equation 12** for geopolymer and **Equation 13** for neat class G cement; Table 1). The cement slurry is injected with a flow rate of 0.2 m/s for 1200 s. The total injected cement slurry is 2.16 m^3 (13.586 bbl). The boundary condition of the outlet is defined as no pressure. Non-slip stationary walls are applied in the interfaces of casing and formation (inner and outer surfaces of the annulus).

3. Results and discussion

The paper compares different performances of neat class G cement and the geopolymer by considering cement volume fraction. The cement volume fraction is calculated by **Equation (14)** (Liu et al., 2001; Dutra et al., 2004). The volume fraction should be 100% if the mud is completely removed. Otherwise, cement is contaminated by the mud, lowering the barrier functionality. When the efficiency is 0%, the domain is full of mud. After hardening, voids and channels are developed, causing gas/fluid migration issues.

The lower cement volume fraction resulting from an incomplete mud removal leads to a high risk of debonding (Renteria et al., 2019). Additionally, the effects of density ratio (Bizhani and Frigaard, 2020), cement injection rate (Xu et al., 2020), and mud contamination on cement (Zheng et al., 2015) are assessed to optimize the pumping process for better, higher quality mud removal. Throughout the paper, the presented snapshots of the displacement results are based on the same volume of the injected cement slurry (cement slurry of 2.16 m^3 is injected).

$$\text{cement volume fraction} = \frac{\text{volume of cement slurry}}{\text{total fluids volume}} \tag{14}$$

3.1. *WBM displaced by neat class G and geopolymer*

Cement volume fraction of the cross-section of cement-formation annulus is studied. The neat class G cement and geopolymer have a good performance in the lower annulus. No residual mud and mud contamination issues are observed in the lower annulus (Fig. 4c). For the upper annulus, cement has a good displacement performance near the casing. At the enlarged section of the wellbore, it is a high risk of having an incomplete drilling fluid removal issue (Fig. 4a). Thus, the cement volume fraction of the middle-enlarged section (black arrows in Fig. 4a present measured location and direction) is shown to evaluate the displacement performance of the neat class G and geopolymer (Fig. 4b). Both cement slurries completely remove WBM within 0.1m away of the casing. As the distance is far from the casing, the displacement performance lowers down. Compared with geopolymer, neat class G has a lower displacement efficiency resulting in a severe mud contamination issue. At the formation interface, the concentrations of neat class G cement and geopolymer are zero indicating a high risk of incomplete displacement induced debonding. Thus, for the enlarged wellbore, two kinds of cement lost well integrity at the formation interface of the upper annulus. Compared with the neat class G cement, the geopolymer can remove more drilling fluid at the same location of the annulus. The following sections evaluate the difference of different cement systems from the inherent property aspect, such as density ratio, flow rate, and mud contaminations.

3.2. *Influence of density ratio*

As presented in Fig. 4, the geopolymer has a better displacement capability than the neat class G cement. To understand the difference, the influence of density ratio, density ratio $= \frac{\text{cement density}}{\text{mud density}}$, is studied. Fig. 5 illustrates the comparison of cement concentration with different density ratios displacing WBM. Density of cement slurry is variable, and other cement properties are the same as neat class G cement.

Bu et al. (2016) investigated the effect of density difference between cement and drilling fluid on displacement efficiency for inclined wells.

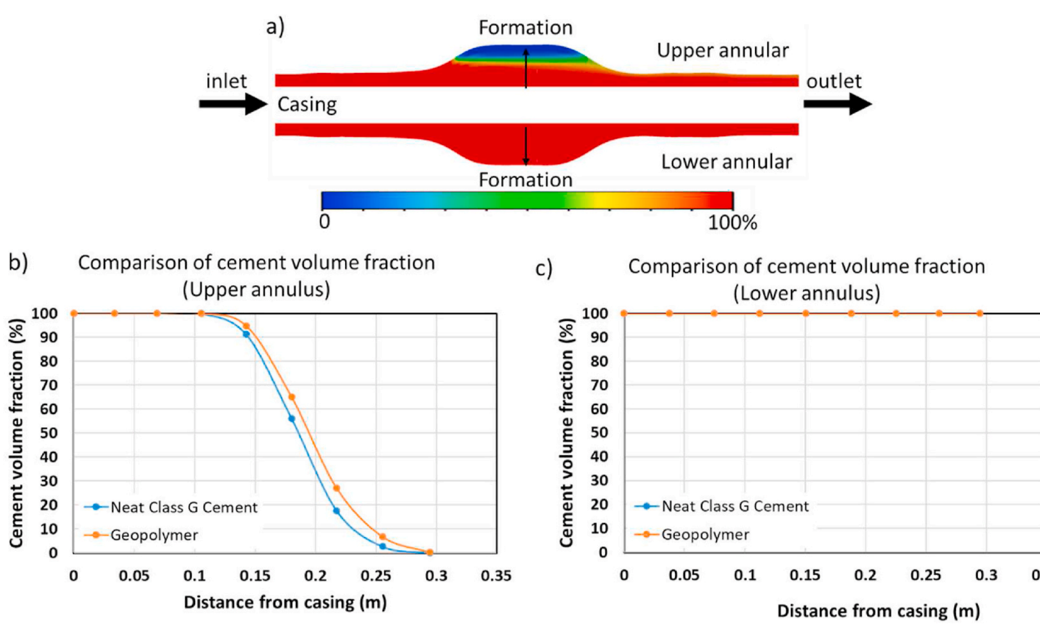

Fig. 4. a) Snapshot of a class G cement-WBM displacement in the annulus. Comparison of cement volume fraction after displacement between neat class G and mud b) in the upper and c) lower annulus.

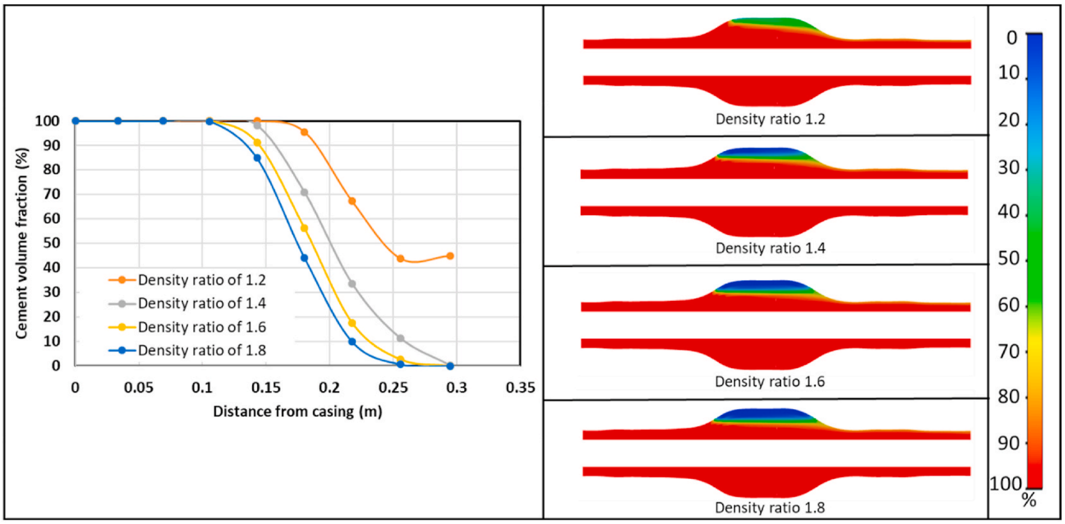

Fig. 5. a) Comparison of cement volume fraction of the middle of the enlarged section in the upper annulus with different density ratios. b) Snapshots of mud displaced by the cement slurries with 1.2, 1.4, 1.6, and 1.8 of density ratios (from top to bottom) after displacement.

As the inclination angle equals 85°, the displacement efficiency decreases when the density ratio is larger than 1.25. However, the study did not discuss horizontal wells or 90° of the angle. This paper aims to fill the knowledge gap. Fig. 5a shows that the lower annulus of all scenarios completely removes the drilling fluid. Mud contamination and residual model issues are in the enlarged section of the upper annulus. The cement slurries concentration is lower as the distance from the casing increases. When a cement slurry with high density displacing WBM because of buoyancy induced by mud-cement density difference, the cement tends to fill from the bottom. The drilling fluid remains at the top of the enlarged section. As the density increases, more residual mud is observed in the upper annulus. For the cases with a density ratio of 1.2 and 1.4, mud contamination happens, while for the density ratio of 1.6 and 1.8, no cement is near the formation interface resulting in an incomplete removal problem (Fig. 5b).

3.3. Influence of cement injection rate

As mentioned before, the flow rate is a controlling parameter in the regular annulus. To extend the research into an enlarged annulus, cement with an injection rate of 0.1, 0.2, 0.3, 0.4, and 0.5 m/s are tested. Mud is completely removed within the 0.06, 0.11, 0.14, 0.15, and 0.17 m from the casing surface with increasing flow rates, respectively. A high risk of debonding is in the scenario with a low flow rate (Fig. 6b). Snapshots (Fig. 6a) show that for the lower flow rate (i.e., cement injected with the rate of 0.1 and 0.2 m/s), the enlarged section and near-outlet of the annulus have mud contamination issues. The increasing injection rates (i.e., cement injected with the rate of 0.3, 0.4, and 0.5 m/s) improve the mud displacement due to a better sweep efficiency.

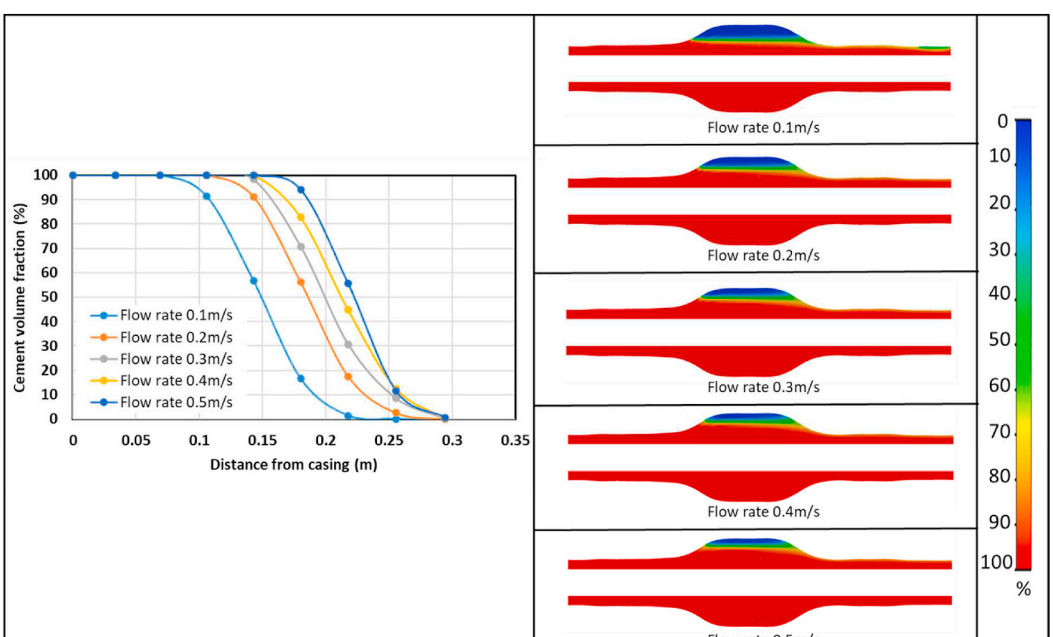

Fig. 6. a) Comparison of cement volume fraction of the middle of the enlarged section in the upper annulus with different flow rates. b) Snapshots of mud displaced by the cement slurries with 0.1, 0.2, 0.3, 0.4, and 0.5 m/s of flow rate (from top to bottom) after displacement.

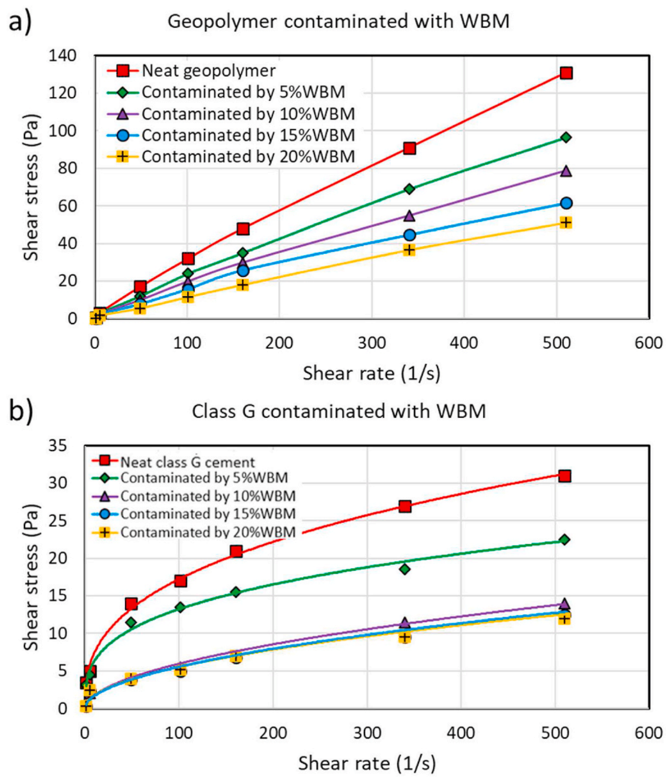

Fig. 7. Relationship between shear stress and shear rate for a) geopolymer and b) class G cement contaminated with different amounts of WBM (Eid et al., 2021).

3.4. *Influence of mud contamination*

Previous studies showed that the circulating and residual mud act as a source of contamination when cement passes later, lowering the displacement efficiency. In this section, different amounts of WBM contaminated cement are assessed. The model is simulated based on flow properties measured in lab experiments. Fig. 7 illustrates the rheology testing results of neat geopolymer, class G cement, and contaminated with WBM (Eid et al., 2021). All the samples show a non-Newtonian shear thinning behavior as their viscosity decreases with an escalation in shear rate due to the length of oligomers formed during conditioning of the slurry. An increasing amount of WBM contamination of both cement systems results in a reducing slurry's viscosity. Both types of cement and contaminated slurries are simulated based on the Herschel-Bulkley non-Newtonian rheological model.

To evaluate the effect of mud contamination, cement slurry contaminated with different amounts of WBM is investigated. Fig. 8 presents the cement volume fraction of the middle point in the enlarged section (red "X" mark) of the upper annulus due to the high risk of lack of cement integrity shown in the last section. The results show a better performance of geopolymer non-contaminated and contaminated cement. For the geopolymer, the cement volume fraction is from 96%, 91%, 87%, 84%, and 77% as 0%, 5%, 10%, 15%, and 20% of WBM contaminations. For the class G cement, the concentration of cement is 82%, 79%, 73%, 70%, and 67%, as the same range of WBM contaminations are applied. WBM contamination has less influence in geopolymer than class G cement. The observation is in agreement with the previous studies investigating regular annuli (Kanesan et al., 2019).

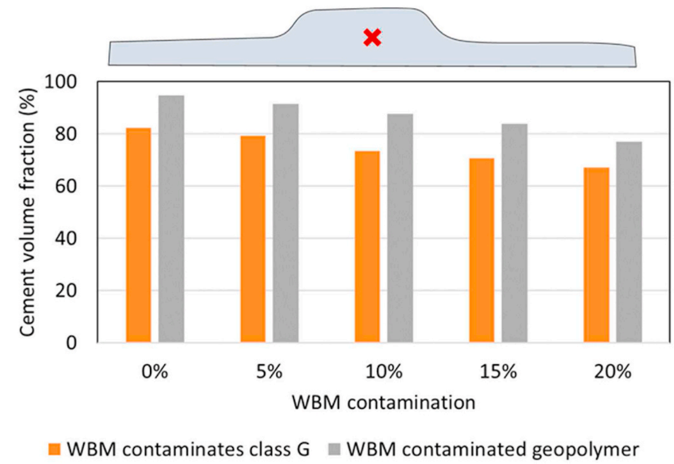

Fig. 8. Cement volume fraction of middle point in the enlarged section (red "X" mark at top) of geopolymer and class G cement contaminated with different amounts of WBM. (For interpretation of the references to colour in this figure legend, the reader is referred to the Web version of this article.)

4. Conclusion

This research improved the study of mud displacement in an enlarged horizontal wellbore. A 3D computational fluid dynamics model was employed to simulate the cement concentration for evaluating the displacement performance in an unconventional formation, TMS. The performance of neat class G cement and rock-based geopolymer was compared. Various scenarios were simulated to assess the influence of density ratio, cement injection rate, and mud contamination on the displacement efficiency.

- Both types of cement (neat class G cement and rock-based geopolymer) have a good performance in the lower annulus. Due to incomplete mud removal, debonding has a high possibility to occur near the formation surface of the upper annulus.
- For the same amount of cement slurry injection, the comparison between geopolymer and neat class G cement shows that the former cement has a high cement volume fraction resulting in a lower risk of cement failure.
- Regardless of changing the mud density, the density of cement slurries significantly influences cement volume fraction. Reducing the density difference (or the density ratio is closed to 1.0) causes few residual drilling fluids in the annulus due to buoyancy effects.
- Neat class G cement with different injection rates is used to test the influence of flow conditions. For the testing range, a high rate leads to a better displacement efficiency. Compared with the density, the flow rate has a lower sensitivity on the cement volume fraction.
- WBM contaminations decrease the quality of geopolymer and class G cement. With the same amount of WBM contamination, geopolymer has a better performance.

Authorship contributions

Yuxing Wu: Modeling and Formal analysis, drafting and revising the manuscript. **Saeed Salehi**: Reviewing and editing the manuscript

Mahmoud Khalifeh: Reviewing and editing the manuscript.

Declaration of competing interest

The authors declare that they have no known competing financial interests or personal relationships that could have appeared to influence the work reported in this paper.

Acknowledgment

The authors would like to extend their gratitude to the Well Construction Technology Center of the University of Oklahoma for providing the necessary resources to publish this work. The authors would also like to thank Research Council of Norway, TOTAL, AkerBP and ConocoPhillips for their supports through the SafeRock project (RCN: #319014 - New Cementitious Material for Oil Well Cementing Applications), and US Department of Energy under award DE-FE0031575 (Tuscaloosa Marine Shale Laboratory) for their supports.

Nomenclature

Abbreviations

CFD	Computational fluid dynamics
TMS	Tuscaloosa Marine Shale
WBM	Water-based mud
OBM	Oil-based mud
HTHP	High-temperature and high-pressure
PISO	Pressure implicit method with splitting of operators

Symbols

$\frac{dV_c}{dy}$	Velocity of slurries along the y-direction
$\frac{dV_m}{dy}$	Velocity of drilling fluids along the y-direction
$\frac{\partial p}{\partial z}$	Friction pressure gradient between fluids and annulus surface
R_e	Reynolds number
T_0	Yield stress
ρ_m	Drilling fluid density
τ_{oc}	Yield stresses of the cement slurry
τ_{om}	Yield stresses of the drilling fluid
$\dot{r}$	Shear rate
ρ_c	Cement density
τ_c	Shear stress of the cement slurry
τ_m	Shear stress of the drilling fluid
a	Distance between the slurry-mud interface to Z-axis
(D_1-D_2) or h	Size of the annulus
k	Consistency coefficient
K_c	Consistency coefficient of the cement
K_m	Consistency coefficient of the mud
n	Liquidity index
n_c	Liquidity index of the cement
n_m	Liquidity index of the mud
v	Fluid velocity
V_c	Velocity of the cement
V_m	Velocity index of the mud
θ	Inclination angle
μ	Fluid dynamic viscosity
ρ	Fluid density
τ	Shear stress

References

Bittleston, S.H., Hassenger, O., 1992. Flow of viscoplastic fluids in A rotating concentric annulus. J. Non-Newtonian Fluid Mech. 42 (1–2), 19–36. https://doi.org/10.1016/0377-0257(92)80002-F.

Bu, Y., Li, Z., Wan, C., Li, H.A., 2016. Determination of optimal density difference for improving cement displacement efficiency in deviated wells. J. Nat. Gas Sci. Eng. 31 (2016), 119–128. https://doi.org/10.1016/j.jngse.2016.03.008.

Dutra, E.S.S., Naccache, M.F., Mendes, P.R.S., Miranda, C.R., Martins, A.L., Campos, G., 2004. Liquid displacement during oilwell cementing operations. Ann. Transact. Nordic Rheol. Soc. 12 (1), 93–100.

Eid, E., Tranggono, H., Khalifeh, M., Salehi, S., Saasen, A., 2021. Impact of drilling fluid contamination on performance of rock-based geopolymers. SPE J. 1–8 https://doi.org/10.2118/205477-PA. SPE-205477-PA.

Enayatpour, S., van Oort, E., 2017. Advanced Modeling of Cement Displacement Complexities. Paper presented at the SPE/IADC Drilling Conference and Exhibition, The Hague, The Netherlands. https://doi.org/10.2118/184702-MS. March 2017. SPE-184702-MS.

Foroushan, H.K., Ozbayoglu, E.M., Gomes, P.J., Yu, M., 2020. Mud/cement displacement in vertical eccentric annuli. SPE Drill. Complet. 35 (2), 297–316. SPE-184702-MS. https://doi-org.ezproxy.lib.ou.edu/10.2118/184702-MS.

Guzman, J., Mavares, F., Monasterios, E., Massirrubi, L., 2018. Casing Centralization and Pipe Movement in Cementing Operations for Improved Displacement Efficiency. In: Paper Presented at the SPE Trinidad and Tobago Section Energy Resources Conference. Port of Spain, Trinidad and Tobago. https://doi.org/10.2118/191255-MS. June 2018. SPE-191255-MS.

Kanesan, D., Chandran, D., Azhar, N.A.B., 2019. Contamination effect of synthetic based mud on fly ash based geopolymer cement slurry. ARPN J. Eng. Appl. Sci. 14 (10), 1871–1875.

Kiran, R., Salehi, S., Mokhtari, M., Kumar, A., 2019. Effect of irregular shape and wellbore breakout on fluid dynamics and wellbore stability. In: Paper Presented at the 53rd U.S. Rock Mechanics/Geomechanics Symposium. New York City, New York, June 2019. ARMA-2019-2058.

Lavrov, A., Torsaeter, M., 2016. Physics and Mechanics of Primary Well Cementing. Trondheim, first ed. Switzerland.

Li, Z., Liu, H., Guo, X., Ou, H., Gu, T., 2016. Contamination of cement slurries with oil based mud and its components in cementing operations. J. Nat. Gas Sci. Eng. 29, 160–168. https://doi.org/10.1016/j.jngse.2016.01.003.

Liu, C., Huang, B., Xu, T., 2001. Theories and Applications of Oil and Gas Well Cementing. China Petroleum Industry Press, Beijing, pp. 292–304.

Liu, X., Nair, S., Aughenbaugh, K., van Oort, E., 2019. Mud-to-Cement conversion of non-aqueous drilling fluids using alkali activated fly ash. J. Petrol. Sci. Eng. 182 (2019), 106242. https://doi.org/10.1016/j.petrol.2019.106242.

Livescu, S., Craig, S., 2017. A critical review of the coiled tubing friction-reducing technologies in extended-reach wells. Part 1: lubricants. J. Petrol. Sci. Eng. 157 (2017), 747–759. https://doi.org/10.1016/j.petrol.2017.07.072.

Martin, M., Latil, M., 1978. Mud Displacement by Slurry during Primary Cementing Jobs-Predicting Optimum Conditions. In: Paper Presented at the SPE Annual Fall Technical Conference and Exhibition. https://doi.org/10.2118/7590-MS. Houston, Texas, October 1978. SPE-7590-MS.

Moroni, N., Ravi, K., Hemphill, T., Salram, P., 2009. Pipe Rotation Improves Hole Cleaning and Cement-Slurry Placement: Mathematical Modeling and Field Validation. In: Paper Presented at the SPE Offshore Europe Oil and Gas Conference and Exhibition. Aberdeen, UK. https://doi.org/10.2118/124726-MS. September 2009. SPE-124726-MS.

Ozbayoglu, M.E., Saasen, A., Sorgun, M., Svanes, K., 2008. Effect of Pipe Rotation on Hole Cleaning for Water-Based Drilling Fluids in Horizontal and Deviated Wells. In: Paper Presented at the IADC/SPE Asia Pacific Drilling Technology Conference and Exhibition. https://doi.org/10.2118/114965-MS. Jakarta, Indonesia, August 2008. SPE-114965-MS.

Pang, B., Wang, S., Jiang, X., Lu, H., 2019. Effect of orbital motion of drill pipe on thetransport of non-Newtonian fluid-cuttings mixture in horizontal drilling annulus. J. Petrol. Sci. Eng. 174 (2019), 201–215. https://doi.org/10.1016/j.petrol.2018.11.009.

Pang, B., Wang, S., Wang, Q., Yang, K., Lu, H., Hassan, M., Jiang, X., 2018. Numerical prediction of cuttings transport behavior in well drilling using kinetic theory of granular flow. J. Petrol. Sci. Eng. 161 (2018), 190–203. https://doi.org/10.1016/j.petrol.2017.11.028.

Renteria, A., Maleki, A., Frigaard, I.A., Lund, B., Taghipour, A., Ytrehus, J.D., 2019. Effects of irregularity on displacement flows in primary cementing of highly deviated wells. J. Petrol. Sci. Eng. 172 (2019), 662–680. https://doi.org/10.1016/j.petrol.2018.08.045.

Richard, C.H., Crook, R.J., 1979. Primary Cementing: the Mud Displacement Process. In: Paper Presented at the SPE Annual Technical Conference and Exhibition. Las Vegas, Nevada. https://doi.org/10.2118/8253-MS. September 1979. SPE-8253-MS.

Savery, M., Darbe, R., Chin, W., 2007. Modeling Fluid Interfaces during Cementing Using a 3D Mud Displacement Simulator. In: Paper Presented at the Offshore Technology Conference. U.S.A., Houston, Texas https://doi.org/10.4043/18513-MS. April 2007. OTC-18513-MS.

Turner, W., Adam, D., Cowan, K.M., Tellez, D., Willis, J., 2019. Casing Rotation for Improved Cement Quality in Unconventional Horizontal Wellbores. In: Paper Presented at the SPE Annual Technical Conference and Exhibition. Calgary, Alberta, Canada. September 2019. SPE-196232-MS. https://doi-org.ezproxy.lib.ou.edu/10.2118/196232-MS.

Xie, L., Chaudhary, S., Chen, Z., 2015. Analysis of the Effect of Eccentricity on Displacement of Non-newtonian Fluids with a Hybrid Method. In: Paper Presented at the SPE Annual Technical Conference and Exhibition. https://doi.org/10.2118/174909-MS. Houston, Texas, USA, September 2015. SPE-174909-MS.

Xu, B., Zhou, S., He, F., Wang, F., Guo, J., 2020. Using particle image velocimetry to evaluate the displacement efficiency of drilling mud in horizontal well cementing. J. Petrol. Sci. Eng. 195 (2020), 107647. https://doi.org/10.1016/j.petrol.2020.107647.

Yeu, W.J., Katende, A., Sagala, F., Ismail, I., 2019. Improving hole cleaning using low density polyethylene beads at different mud circulation rates in different hole angles. J. Nat. Gas Sci. Eng. 61, 333–343. https://doi.org/10.1016/j.jngse.2018.11.012.

Zheng, Y., She, C., Yao, K., Guo, X., Zhang, H., Yang, T., Li, M., 2015. Contamination effects of drilling fluid additives on cement slurry. Nat. Gas. Ind. 2 (4), 354–359. https://doi.org/10.1016/j.ngib.2015.09.009.